Available online at www.sciencedirect.com
ScienceDirect
Journal of Hazardous Materials 142 (2007) 639–646
Journal of Hazardous Materials
www.elsevier.com/locate/jhazmat

The reactivity of sodium borohydride with various species as characterized by adiabatic calorimetry

N.O. Gonzales, M.E. Levin *, L.W. Zimmerman

Shell Global Solutions (US) Inc., United States

Available online 1 September 2006

Abstract

The reactivity of sodium borohydride in the presence of other species has been examined by adiabatic calorimetry. In combination with water, sodium borohydride exhibits an exotherm at room temperature accompanied by generation of gas (presumed to be hydrogen). Addition of potassium hydroxide to a sodium borohydride–water mixture is found to stabilize the solution and require a higher temperature for reaction to occur. However, if iron oxide is also included, reaction takes place near room temperature. Very rapid reaction was found when a metal chloride was brought in contact with a solution containing sodium borohydride, water, and potassium hydroxide. When sodium borohydride was added to an oxygenated hydrocarbon, reaction at room temperature also took place, but to a more limited extent. Peak temperatures above 200 °C and maximum pressures in excess of 2000 psia were observed in most cases. Kinetics extracted from the calorimetry data are presented for some of the sodium borohydride combinations.

1. Introduction

Sodium borohydride is an effective reducing agent and is used to reduce both organic and inorganic species [1]. However, it is such an effective reducing agent that it is also susceptible to decomposition. It is well known that sodium borohydride can decompose upon exposure to water, releasing hydrogen and heat [2]. The literature also shows that a sodium borohydride/water solution will evolve heat and hydrogen at room temperature. Furthermore, the literature notes that a caustic sodium borohydride solution is less susceptible to sodium borohydride decomposition than a neutral solution.

This readiness to decompose has led to several incidents in the chemical industry where lives were lost and/or property was destroyed. Most notably, in June 1999, there was an explosion at a Finnish Chemical's Aetsa sodium borohydride plant [3]. The explosion leveled one of three reactors during a maintenance shutdown of a new, undisclosed process and led to a fatality.

To fill the gaps in the knowledge of sodium borohydride reactivity with water and with other species, the present study investigates, through use of adiabatic calorimetry, the reactivity of the following combinations:

- sodium borohydride in water,
- sodium borohydride with potassium hydroxide in water,
- sodium borohydride with potassium hydroxide and iron oxide in water,
- sodium borohydride with potassium hydroxide and metal chloride in water,
- sodium borohydride with an oxygenated hydrocarbon.

The approach of measuring kinetics through heat release and pressure generation provides the opportunity to observe and characterize in a laboratory setting the accelerating reaction environment that might be experienced in a commercial-scale incident.

2. Experimental

2.1. Equipment

Testing for this study was carried out in the Automatic Pressure Tracking Adiabatic Calorimeter (APTAC^{TM}) available from TIAX, Inc. The instrument is designed to allow a laboratory-scale sample undergoing an exothermic reaction to self-heat at a rate and extent comparable to that in a commercial-scale, adiabatic environment. This is accomplished by heating the gas space surrounding the sample cell to match the sample temperature, thereby minimizing the heat loss from the sample

* Corresponding author. Tel.: +1 281 544 7575; fax: +1 281 544 7705.
E-mail address: marc.levin@shell.com (M.E. Levin).

0304-3894/$ – see front matter © 2006 Published by Elsevier B.V.
doi:10.1016/j.jhazmat.2006.08.058

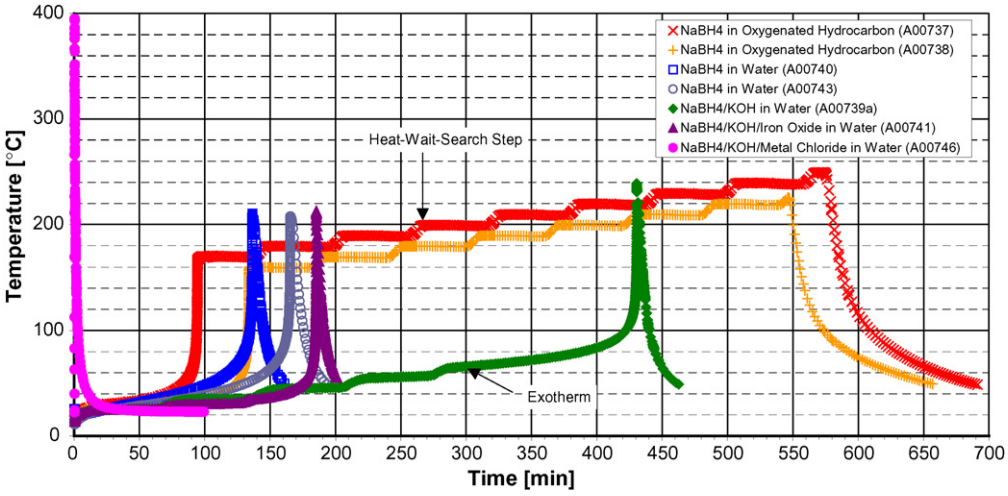

Fig. 1. Temperature history of sodium borohydride solutions in the APTAC.

and sample cell. Balancing of the pressure outside of the sample cell to match the internal pressure of the sample cell enables the apparatus to probe sample pressures as high as 2000 psig without resorting to a thick-walled sample container. This feature, along with the 130 cm^3 spherical sample cell capacity, provide for a low thermal inertia factor, ϕ (expressing the amount of heat absorbed by the sample plus container relative to the sample):

$$\phi = 1 + \frac{m_c Cp_c}{m_s Cp_s}$$

where m denotes the mass, Cp the heat capacity, subscript c the cell + stir bar, and s the sample. Values of ϕ in the APTAC are typically 1.15–1.30.

The APTAC can match temperature and pressure rise rates of up to 400 °C/min and 10,000 psi/min, respectively. Operation is automated and typically starts in the heat-wait-search mode with an exotherm detection threshold of 0.05–0.06 °C/min. Stirring is accomplished via a Teflon-coated magnetic stir bar inserted in the sample cell.

More details about the operating principles, construction, and operation of the APTAC have been described previously [4].

2.2. Samples

Materials for this study, sodium borohydride (catalog #48,088-6), potassium hydroxide (catalog #30,656-8), iron oxide, and metal chloride, were obtained from Sigma–Aldrich. The oxygenated hydrocarbon was purchased from GAF Chemicals. In the experiments containing water, de-ionized water was employed.

2.3. Procedures

To preclude reaction of sodium borohydride with water outside of the sample cell, the sodium borohydride, metal chloride, iron oxide and potassium hydroxide samples were handled and loaded into the sample cell in a nitrogen-purged glove box, which kept the relative humidity below 15%. The sample cell was capped with the septum in the glove box and transferred to a glove bag. After the glove bag was attached to the APTAC containment vessel head and purged with five vacuum/nitrogen cycles, the septum was then removed from the sample cell and the sample cell was attached to the vessel head. Once the sample cell was mounted on the APTAC and the containment vessel closed, chilled water was manually injected via syringe into the cell to start the experiment. In the experiment containing metal chloride, a chilled water solution of metal chloride was prepared and then injected into a sample cell containing sodium borohydride and potassium hydroxide. In the sodium borohydride/oxygenated hydrocarbon experiments, both components were loaded into a sample cell prior to mounting the cell to the APTAC.

A summary of test characteristics may be found in Table 1. Note that no gas samples for compositional analysis were taken at the end of any of the tests.

Total sample weights ranged from 30 to 44 g while the total weight of the titanium cell and stir bar ranged between 32.9 and 36.1 g.

3. Results and discussion

3.1. Sodium borohydride in water

It is known that sodium borohydride will decompose when contacted with water to give sodium metaborate ($NaBO_2$) and hydrogen [2]. Furthermore, upon decomposition, one mole of sodium borohydride will generate four moles of hydrogen gas and liberate 59.5 kcal of heat [5]. It is this pressure and heat generation that is of concern when handling and using sodium borohydride.

Experiments were sought to probe the reactivity of a sodium borohydride/water solution under adiabatic conditions. The sodium borohydride/water experiment in the APTAC also serves as a baseline for use in further experiments containing "contaminants". For a sodium borohydride concentration of 12 wt.% in water, the APTAC experiments revealed reaction at approximately 20 °C, as shown in Fig. 1, which plots sample temperature versus time. Fig. 1 also shows that the sodium borohydride/water

Table 1
Summary of APTAC test conditions and results for sodium borohydride decomposition

	Run ID						
	A00740	A00743	A00739a	A00741	A00746	A00737	A00738
Sodium borohydride mass (g)	3.6	3.6	3.6	3.62	3.6	2.75	2.74
Water mass (g)	26.34	26.38	26.34	26.34	27.05	–	–
Potassium hydroxide mass (g)	–	–	0.90	0.90	0.95	–	–
Iron oxide mass (g)	–	–	–	1.02	–	–	–
Metal chloride mass (g)	–	–	–	–	8.23	–	–
Oxygenated hydrocarbon mass (g)	–	–	–	–	–	40.02	41.29
Total sample mass (g)	29.94	29.98	30.84	31.88	39.83	42.77	44.03
Sodium borohydride percentage (wt.%)	12.0	12.0	11.7	11.4	9.0	6.4	6.2
Potassium hydroxide percentage (wt.%)	–	–	2.9	2.8	2.4	–	–
Sample pad gas	Nitrogen	Nitrogen	Nitrogen	Nitrogen	Nitrogen	Nitrogen	Nitrogen
Sample cell mass (g)	32.18	32.64	29.36	32.06	31.90	32.25	32.24
Sample cell material	Titanium	Titanium	Titanium	Titanium	Titanium	Titanium	Titanium
Stir bar mass (g)	3.45	3.47	3.49	3.54	3.49	3.38	3.40
Stirring rate (magnetic) (rpm)	500	500	500	500	500	500	500
Expt (search) start temperature (°C)	20	23	25	25	25	30	25
Heat-wait-search increment (°C)	5	5	10	5	5	10	5
Expt duration (before S/D) (min)	161	193	458	201	99	691	657
Expt temperature shutdown (°C)	450	450	450	450	450	450	450
Expt pressure shutdown (psia)	1900	1900	1900	1900	1800	1900	1900
Expt heat rate shutdown (°C/min)	2000	2000	2000	2000	2000	2000	2000
Expt pressure rate shutdown (psi/min)	10,000	10,000	10,000	10,000	10,000	10,000	10,000
Exotherm threshold (°C/min)	0.05	0.05	0.05	0.05	0.05	0.05	0.05
Number of exotherms	1	1	1	1	1	1	1
Approximate onset temperature (0.05 °C/min) (°C)[a]	24	24	63	15	≤22	15	14
Max observed temperature (°C)	210	208	239	213	395	170	160
Max observed pressure (psi)	2025	2000	2112	1998	1275	1455	1450
Max observed self-heat rate (°C/min)	357	294	910	2350[b]	9840[b]	250	159
Max observed pressure rate (psi/min)	5280	4190	14,600[b]	31,900[b]	24,100[b]	2800	2000
Temp at max self-heat rate (°C)	191	192	236	204	343	154	145
Temp at max pressure rate (°C)	197	194	220	204	345	150	144
Thermal inertia, ϕ	1.16	1.16	1.15	1.16	1.15	1.22	1.21
Estimated gas generated (mol/mole $NaBH_4$)[c]	3.7	3.4	3.3	3.3	–	3.1	3.2
Estimated heat of reaction (kcal/gmol $NaBH_4$)	68.7	68.7	67.4	74.4	187	63.1	60.1
Expt shutdown cause	Over pressure	Over pressure	Over pressure	Over pressure	Manual S/D	Manual S/D	Manual S/D

[a] By extrapolation of the self-heat rate data (ignoring possible negative or positive drift).
[b] Self-heat and pressurization rates sufficiently high to cause possible temperature, pressure-reading lags.
[c] Considering peak pressure as non-condensibles, accounting for the temperature and gas cap volume at peak pressure.

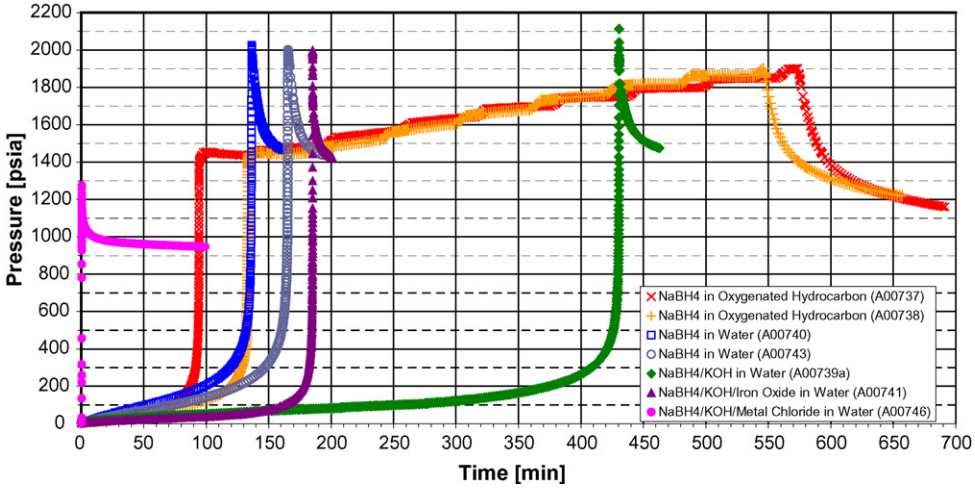

Fig. 2. Pressure history of sodium borohydride solutions in the APTAC.

solution eventually reaches a maximum temperature of 210 °C. The sample pressure, as plotted in Fig. 2, also indicates that reaction occurs shortly after contact, with a final sample pressure over 2000 psia. An estimate of the number of moles of gas generated per mole of sodium borohydride is presented in Table 1. This estimate assumes that the pressure arises entirely from non-condensible gas and it accounts for the effect of temperature at the peak pressure and the approximate gas cap in the cell (based on thermal expansion of the liquid). In this case, 3.7 moles of gas were generated per mole of sodium borohydride, compared with the expected 4.0.

The qualitative kinetic behavior of the sample is illustrated in the self-heat rate plot in Fig. 3. This graph displays temperature rise rate versus negative reciprocal temperature (with the corresponding temperatures in °C shown). The direct link to an Arrhenius plot can be obtained by multiplying the self-heat rate by the sample heat capacity and dividing by the heat of reaction to yield the observed reaction rate. Fig. 4 displays the same information as Fig. 3, except that the initial heat-wait-search steps have been removed for clarity. As can be seen in Fig. 4, the onset temperature, defined for the APTAC as the temperature at which the temperature rise rate is 0.05 °C/min, is approximately 20 °C. Fig. 4 also shows the maximum rate of heat generation to be 360 °C/min. It is not clear whether the low level, relatively temperature-independent self-heat rate behavior below 40 °C is the result of positive instrument drift or some other reaction occurring in these conditions.

The maximum pressure generation rate is 5300 psi/min, as can be seen in Fig. 5. Also, the final pressure in the sample cell is approximately 1500 psi when the sample cools to 50 °C, as shown in Fig. 6, confirming that non-condensable gases have been generated. Finally, Fig. 7 shows the time to maximum reaction rate at a given temperature. Reading from Fig. 7, for example, a sodium borohydride/water mixture at approximately 70 °C will reach its maximum reaction rate in 10 min.

In addition to obtaining calorimetric data, kinetics were extracted for the decomposition of sodium borohydride. Modeling of the reaction dynamics, taking into account fluid properties (temperature dependent where appropriate) as well as the heat absorbed by the sample cell and stir bar (but with constant cell/stir bar heat capacity), was accomplished via the software, SAFIRE, from the American Institute of Chemical Engineers. Visual fitting of the self-heat rate data indicates a reaction that is slightly less than first-order in sodium borohydride concentration. Under neutral conditions, the following kinetics apply:

$$\text{rate}\,(\text{kmol/m}^3\text{s}) = A\exp\left[\frac{-E_a}{RT}\right][\text{NaBH}_4]^{0.7}$$

where[$NaBH_4$] = concentration of sodium borohydride in kmol/m^3, $A = 5.8 \times 10^7$ (kmol)$^{0.3}$ (m^3)$^{-0.3}$ s^{-1}, E_a = 17,950 cal/gmol, R = 1.9872 cal/mol K, and T in Kelvin.

A heat of reaction of 69.9 kcal/gmol is necessary to fit the observed adiabatic temperature rise. This value is somewhat higher than the reported value given earlier for formation of sodium metaborate from sodium borohydride.

Note that these are lumped kinetics and are representative of the sum of possibly many discrete reactions occurring in the sample.

3.2. Sodium borohydride with potassium hydroxide in water

It is also known that potassium hydroxide will stabilize a sodium borohydride solution against thermal decomposition, but the high temperature characteristics of the solution were not well described in the literature [6]. Using similar concentrations to the previous sodium borohydride/water experiments, a mixture containing 11.7 wt.% sodium borohydride and 2.9 wt.% potassium hydroxide was examined. In Figs. 1 and 2, the temperature and pressure do not appreciably rise until the sample reaches the 60–70 °C range. (Compare to an observable temperature rise at ~20 °C for a sodium borohydride/water solution.) These results imply that potassium hydroxide stabilizes a low concentration sodium borohydride solution so that it could be handled more safely at ambient temperatures. However, once the temperature reaches 60 °C, the reaction proceeds to a maximum temperature of 240 °C and a maximum pressure greater than 2100 psi, as seen in Figs. 1 and 2.

Fig. 4 clearly shows the onset of reaction to be 60 °C (at a 0.05 °C/min rate). Again, the higher onset temperature reflects the stabilizing influence of the potassium hydroxide in the sodium borohydride/water solution. Fig. 4 also shows that the maximum rate of heat generation to be 900 °C/min, higher than the sodium borohydride/water solution, which is due to the higher onset temperature and activation energy(slope). On the other hand, the final sample pressure at 50 °C (after reaction is complete) is approximately 1500 psi, an indication of non-condensable gas generation and similar to the sodium borohydride/water samples. Fig. 7 shows the time to maximum reaction rate, which, for a given temperature, is considerably longer than the sodium borohydride/water samples tested, another reflection of the fact that potassium hydroxide stabilizes the sodium borohydride/water solution.

In addition to obtaining calorimetric data on this mixture, kinetics were extracted for the decomposition of a sodium borohydride/potassium hydroxide/water solution. Again, the reaction rate was found to be slightly less than first-order in sodium borohydride concentration by visually fitting the data. Under the particular basic conditions of the test, the following kinetics apply:

$$\text{rate}\,(\text{kmol/m}^3\text{s}) = A\exp\left[\frac{-E_a}{RT}\right][\text{NaBH}_4]^{0.7}$$

[$NaBH_4$] is the concentration of sodium borohydride in kmol/m^3, $A = 2.4 \times 10^{10}$ (kmol)$^{0.3}$ (m^3)$^{-0.3}$ s^{-1}, E_a = 24,000 cal/gmol, R = 1.9872 cal/mol K, and T in Kelvin.

A 69.9 kcal/gmol heat of reaction is consistent with the observed adiabatic temperature rise.

Note that these are lumped kinetics and are representative of the sum of possibly many discrete reactions occurring in the sample.

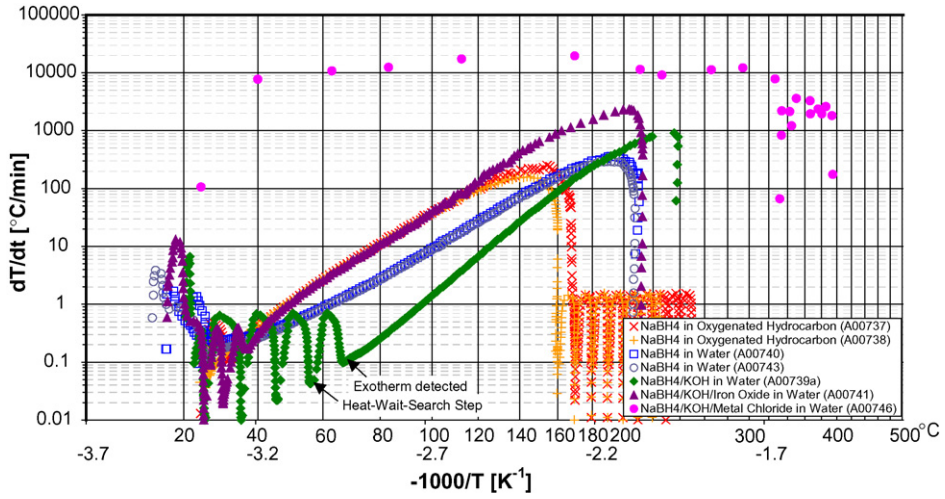

Fig. 3. Self-heat rate–temperature profiles of sodium borohydride solutions in the APTAC.

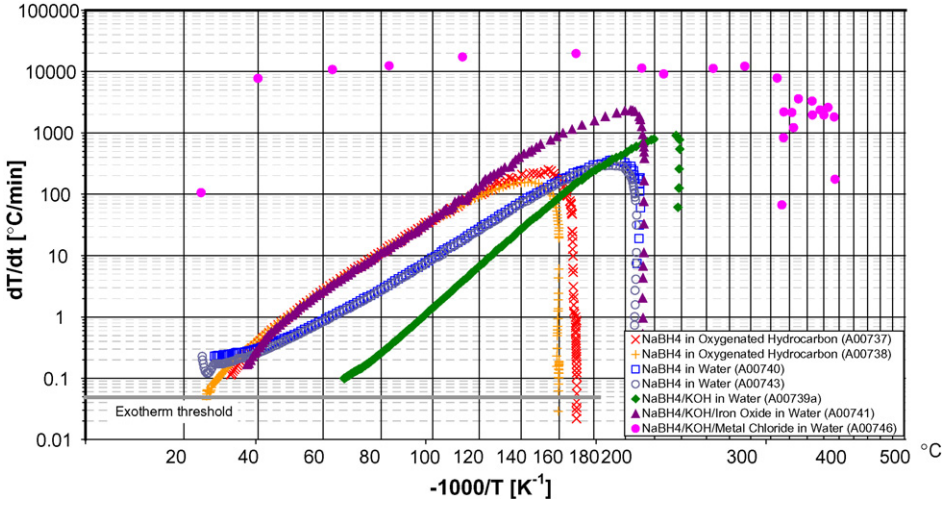

Fig. 4. Self-heat rate–temperature profiles of sodium borohydride solutions in the APTAC; heat-wait-search steps removed.

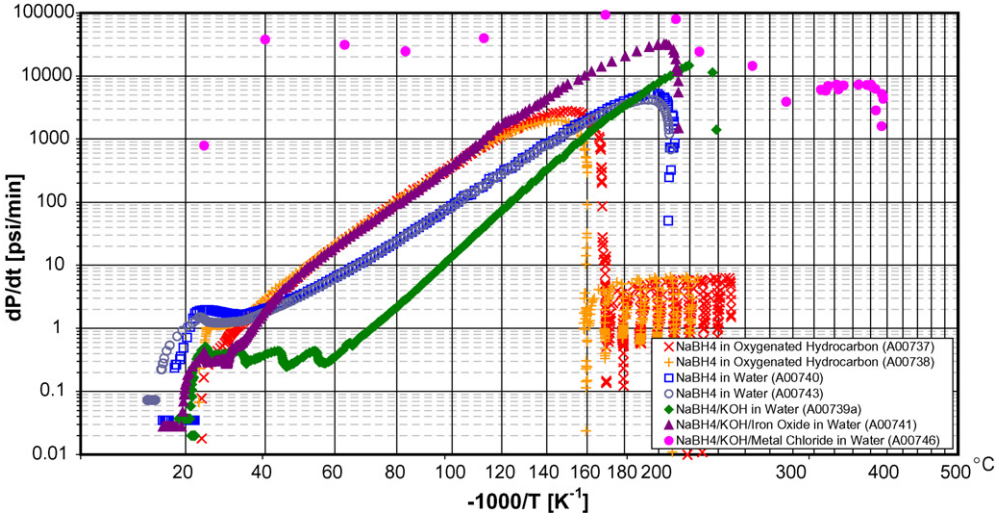

Fig. 5. Pressurization rate–temperature profiles of sodium borohydride solutions in the APTAC.

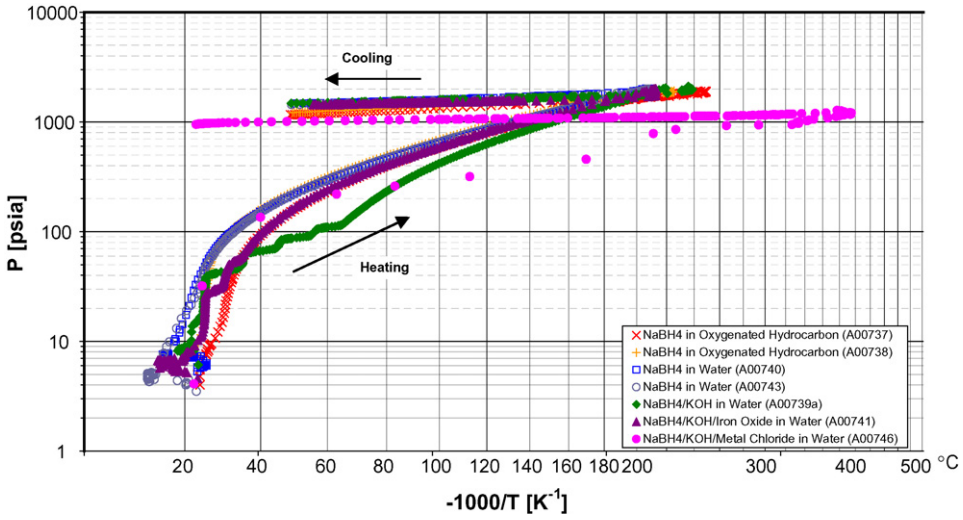

Fig. 6. Pressure–temperature profiles of sodium borohydride solutions in the APTAC.

3.3. Sodium borohydride, potassium hydroxide, and iron oxide in water

The combination of a sodium borohydride/potassium hydroxide solution with iron oxide was investigated since this contacting is possible in a manufacturing process. The experimental test solution contained 11.4 wt.% sodium borohydride, 2.8 wt.% potassium hydroxide, and 3.2 wt.% iron oxide. Again, these solid materials were added to the sample cell and then chilled water was injected via syringe. Figs. 1 and 2 show temperature and pressure increases just above room temperature with a maximum temperature of 210 °C and a maximum pressure of 2000 psi. By inspection of the self-heat rates at the *bottom* of the initial heat-wait-search steps in Fig. 3 (at 25 and 30 °C), a dramatic rise in reactivity with increasing temperature is noted. It is not known if this is merely negative instrument drift or the occurrence of autocatalytic behavior. Fig. 4 shows that the mixture reacts around room temperature for a 0.05 °C/min rate, a clear indication that iron oxide decreases the stability of a sodium borohydride/potassium hydroxide/water solution. Furthermore, Fig. 4 also highlights a maximum heat generation rate of 2350 °C/min, much higher than that for sodium borohydride/water solutions and for sodium borohydride/potassium hydroxide/water solutions. As with the previous samples, the final sample pressure at 50 °C (after reaction is complete) is approximately 1500 psi, a sign that non-condensable gases were generated. Fig. 7 gives the time to maximum reaction rate for the solution and shows that the iron oxide-containing solution has a higher reactivity than sodium borohydride/water and sodium borohydride/potassium hydroxide/water solutions.

Note that other forms of iron oxide may or may not catalyze sodium borohydride decomposition and only experiments will be able to discern the effects of these different iron oxides on sodium borohydride decomposition.

3.4. Sodium borohydride, potassium hydroxide, and metal chloride in water

The open literature states that metal salts can catalyze or even participate in sodium borohydride decomposition [7–10]. To investigate this, a metal chloride was added to a sodium borohydride/potassium hydroxide solution. The solution tested

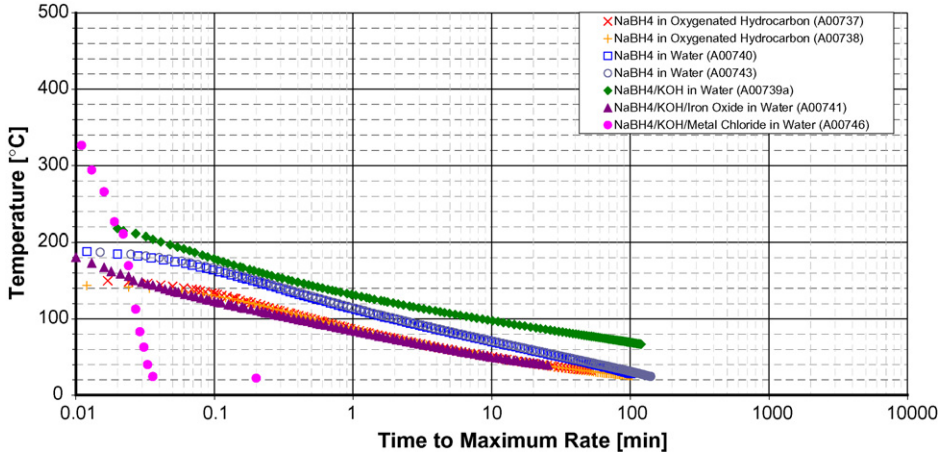

Fig. 7. Time-to-maximum rate profiles of sodium borohydride solutions in the APTAC.

contained 9.0 wt.% sodium borohydride, 2.4 wt.% potassium hydroxide, and 20.7 wt.% metal chloride. To facilitate the transfer of material and to ease concerns about solid–solid reactivity, a metal chloride/chilled water solution was prepared and injected into the sample cell. This test shows a *very* rapid increase in temperature, pressure, and rate of heat generation. A maximum temperature of 400 °C and a maximum pressure of 1300 psi are reached within seconds of exposing the solid material to the metal chloride/water solution, as can be seen in Figs. 1 and 2. The maximum rate of heat generation, see Fig. 4, is greater than 10,000 °C/min. The shape of the curve in Fig. 4 is unusual and may be due to poor heat and mass transfer between the liquid and solid phases as well as between the sample and the thermocouple. Clearly, the presence of a metal chloride boosts sodium borohydride decomposition to the extent that such contact raises a serious safety concern. Furthermore, this enhancement of sodium borohydride decomposition by a metal chloride was new information for some of our staff.

3.5. Sodium borohydride in an oxygenated hydrocarbon

The combination of sodium borohydride and an oxygenated hydrocarbon was also probed. The sodium borohydride/oxygenated hydrocarbon combination was not expected to react significantly at room temperature based on many years of process experience. However, when a sodium borohydride solution of 6.3 wt.% strength in this hydrocarbon was allowed to reach room temperature, the temperature rose and reached a maximum of 170 °C and the pressure reached a maximum of 1450 psi, as shown in Figs. 1 and 2. These notably lower maximum temperatures and pressures are due to smaller amounts of sodium borohydride used (2.75 g in the oxygenated hydrocarbon experiments versus 3.6 g in other experiments). Fig. 4 reveals that the reaction occurs at ambient conditions and achieves a maximum heat generation rate of 250 °C/min. The final sample pressure at a cool-down temperature of 50 °C is approximately 1200 psi, an indication that non-condensable gases were generated. Lastly, Fig. 7 gives the time to maximum reaction rate for the sodium borohydride/oxygenated hydrocarbon solution and shows that this combination has a somewhat higher reactivity than sodium borohydride/water and a much higher reactivity than sodium borohydride/potassium hydroxide/water solutions.

3.6. Thermal inertia effects

In this study's experiments, the thermal inertia or phi factor, ϕ, ranges between 1.15 and 1.22 (see Table 1). This means that the sample container has a thermal capacitance of 15–22% of that of the sample, or expressed differently, about 13–18% of the total of the cell plus sample. The *actual* temperature rise experienced in a large-scale adiabatic environment, in which the *relative* wall thermal capacitance might be very small, would be higher by the thermal inertia factor or an additional 15–22%. Thus, the extent of the each exotherm would be greater. Furthermore, a greater pressure build-up can be expected to accompany the increased temperature rise.

In addition to the impact of thermal inertia on exotherm temperature rise, the self-heat rates associated with the exotherms would be greater at the commercial scale than those observed in the experiments by a factor larger than the thermal inertia factor. This means that the timeframe for a temperature/pressure excursion beginning at some initial temperature would be correspondingly shorter. To adjust the current study's results properly for equipment with a lower thermal inertia, a dynamic simulation that takes into account the observed reaction kinetics coupled with material and equipment properties would be required.

3.7. Sensitivity considerations

Reactions following Arrhenius-type kinetics will exhibit ever-lower self-heat rates as the temperature is lowered. Instead of predicting a reaction to "shut off" at some low temperature, it may be more reasonable to picture the generation of heat from the reaction being "masked" by equipment heat losses or other phenomena (e.g., agitation energy input).

As instrument design and detection limits improve, onset temperatures for reactions can be expected to fall. The lower limit of detection for an exothermic reaction in the APTAC is quoted at 0.04 °C/min. This is generally considered to be near the state-of-the-art (e.g., 0.02 °C/min for the Accelerating Rate Calorimeter™) for laboratory-scale adiabatic calorimeters. Nevertheless, when interpreting raw or thermal inertia-adjusted onset rates, it is important to recognize that rates at even the best laboratory-scale detection limit might be unacceptable in commercial-scale applications. For example, a 0.04 °C/min rate in the APTAC corresponds to a 58 °C/day self-heat rate (with *no* heat losses to the surroundings). A piece of equipment in an operating facility experiencing a heating rate of this magnitude would likely necessitate some form of intervention. In short, care must be exercised when referencing reaction onset temperatures. Such onset temperatures usually do *not* necessarily represent a lower threshold below which reaction does not occur.

4. Conclusions

Using adiabatic calorimetry, an investigation of the reactivity of mixtures of sodium borohydride with various species reveals some unexpected results. Sodium borohydride decomposition in water has been studied previously and the APTAC results confirm that the solution reacts at room temperature. The APTAC reveals new aspects of the reactivity such as a maximum temperature of 210 °C and a maximum pressure of over 2000 psia. Furthermore, the stabilizing effect of potassium hydroxide on sodium borohydride decomposition was known, but APTAC experiments establish the temperature at which the solution displays observable decomposition as approximately 60 °C with the solution reaching a maximum temperature of 240 °C and a maximum pressure over 2100 psia.

However, the increased rate of sodium borohydride decomposition in the presence of iron oxide or a metal chloride was unexpected. These mixtures react at room temperature and give final temperatures over 200 °C and final pressures over 1200 psi.

Finally, the reactivity of sodium borohydride with an oxygenated hydrocarbon was probed. This mixture also reacts at room temperature, leading to a final temperature of over 160 °C and a final pressure of over 1400 psia.

Finally, combining sodium borohydride with solvents and/or other materials, in light of its sensitivity to decomposition, could result in rapid temperature and pressure rises under unexpected circumstances. Testing should be performed to assess the potential chemical incompatibility of these novel (and sometimes inadvertent) combinations.

References

[1] Kirk-Othmer Encyclopedia of Chemical Technology, vol. 13, 4th ed., John Wiley & Sons, New York, 1995.
[2] F.A. Cotton, G. Wilkinson, Advanced Inorganic Chemistry, 5th ed., John Wiley & Sons, New York, 1988.
[3] Chemical Week, vol. 161, no. 23, June 16, 1999, p. 8.
[4] M.E. Levin, A.D. Hill, Reactivity of unsaturated hydrocarbons via adiabatic calorimetry, in: Proceedings of the 2000 Mary Kay O'Connor Process Safety Center Annual Symposium, 2000.
[5] D.D. Wagman, et al., The NBS tables of chemical thermodynamic properties, selected values for inorganic and C1 and C2 organic substances in SI units, J. Phys. Chem. Ref. Data vol. 11 (Suppl. 2) (1982).
[6] Ullmann's Encyclopedia of Industrial Chemistry, vol. 16, 6th ed., Wiley–VCH, Germany, 2003.
[7] N.I. Sax, R.J. Lewis Sr., Dangerous Properties of Industrial Materials, 7th ed., Van Nostrand Reinhold, New York, 1989.
[8] K.A. Holbrook, P.J. Twist, J. Chem. Soc. (A) (1971) 890.
[9] G.N. Glavee, K.J. Klabunde, C.M. Sorensen, G.C. Hadjapanayis, Langmuir vol. 8 (1992) 771–773.
[10] R.C. Wade, D.G. Holah, A.N. Hughes, B.C. Hui, Catal. Rev. Sci. Eng. 14 (1976) 211.